

RSC Advances



This is an *Accepted Manuscript*, which has been through the Royal Society of Chemistry peer review process and has been accepted for publication.

Accepted Manuscripts are published online shortly after acceptance, before technical editing, formatting and proof reading. Using this free service, authors can make their results available to the community, in citable form, before we publish the edited article. This *Accepted Manuscript* will be replaced by the edited, formatted and paginated article as soon as this is available.

You can find more information about *Accepted Manuscripts* in the [Information for Authors](#).

Please note that technical editing may introduce minor changes to the text and/or graphics, which may alter content. The journal's standard [Terms & Conditions](#) and the [Ethical guidelines](#) still apply. In no event shall the Royal Society of Chemistry be held responsible for any errors or omissions in this *Accepted Manuscript* or any consequences arising from the use of any information it contains.



Effects of pH Value and Temperature on the Initiation, Promotion, Inhibition and Direct Reaction Rate Constants of Natural Organic Matter in Ozonation

Received 00th January 20xx,
Accepted 00th January 20xx

DOI: 10.1039/x0xx00000x

www.rsc.org/

Ee Ling Yong^a and Yi-Pin Lin^b

The effects of pH value and temperature on the initiation (k_i), promotion (k_p), inhibition (k_s) and direct ozone reaction (k_D) rate constants of natural organic matter (NOM) in water ozonation were investigated in this study. These rate constants were determined using a newly developed method that integrates the classical R_{ct} concept, the transient steady-state hydroxyl radical ($\cdot\text{OH}$) concentration model and the pseudo first-order ozone decomposition model. Suwannee River fulvic acid (SRFA) was selected as the model NOM. Our results showed that (1) the variation of pH value from 6.5–8.0 had little influence on k_p ; while k_i showed a peak value at pH 7.5, and k_s and k_D increased with the increasing pH, (2) at room temperature, the value of k_D is 2.7–5.8 times higher than k_i and that of k_p is 14–31 times higher than k_s at pH 6.5–8.0, indicating that direct ozone reaction and promotion reaction are the dominant pathway for SRFA to react with ozone and $\cdot\text{OH}$, respectively, and (3) all rate constants showed a strong dependency on temperature and the activation energies for initiation, promotion, inhibition and direct ozone reaction were determined to be 55.3, 25.6, 50.1 and 49.1 kJ mol⁻¹, respectively. Functional groups in NOM that are potentially responsible for these reactions were discussed. Our results provide deeper insights of the reactions between NOM and ozone/ $\cdot\text{OH}$ and the removal of micropollutants in ozonation process can be evaluated using the rate constants determined in this study.

1. Introduction

The use of ozone (O_3) in advanced drinking water treatment has been increasing over the past several decades. Ozonation is effective both in the inactivation of pathogens^{1–5} and removal of organic contaminants^{6–8}. Its use for emerging contaminant degradation in wastewater has also been demonstrated^{9–11}.

O_3 is a strong oxidant that selectively attacks the electron-rich moieties of a compound¹². It decomposes in natural water primarily due to its reactions with hydroxide ions (OH^-) and natural organic matter (NOM)^{8, 13}. The reaction between O_3 and OH^- can lead to the formation of hydroxyl radical ($\cdot\text{OH}$), a non-selective and stronger oxidant than O_3 ^{14, 15}. Both O_3 and $\cdot\text{OH}$, therefore, should be considered in the removal of contaminants in the ozonation process¹⁶. NOM is present ubiquitously in natural water systems¹⁷. It can react directly with O_3 molecule and participate in reactions characterized as initiation, promotion and inhibition depending on the net production and consumption of $\cdot\text{OH}$ ^{13, 18, 19}. Determination of the rate constants of NOM in these reactions is highly desirable because the influences of NOM on the degradation of organic contaminants by ozonation can then be quantified.

We recently developed a new method that can be used to

determine the rate constants of NOM in these reactions^{20, 21}. This method requires the addition of different concentrations of an external inhibitor (denoted as S with a second-order rate constant k_{SS} with $\cdot\text{OH}$) such as *tert*-butanol into the experimental solution. By integrating the R_{ct} concept²², the transient steady-state $\cdot\text{OH}$ concentration model¹³ and the pseudo first-order ozone decomposition model¹³, the following two equations can be established for a carbonate-free system:

$$\frac{1}{R_{ct}} = \frac{k_{SS}[S] + k_S[\text{DOC}]}{2k_1[\text{OH}^-] + k_i[\text{DOC}]} \quad (1)$$

$$-\frac{d[\text{O}_3]}{dt} \cdot \frac{1}{[\text{O}_3]} = k_{\text{obs}} = 3k_1[\text{OH}^-] + k_D[\text{DOC}] + k_i[\text{DOC}] + k_p[\text{DOC}]R_{ct} \quad (2)$$

where R_{ct} is the ratio of $\cdot\text{OH}$ exposure to ozone exposure, k_1 is the second-order rate constant between OH^- and O_3 , $[\text{DOC}]$ is the dissolved organic carbon concentration, k_i , k_p , k_s and k_D denote the DOC-normalized initiation, promotion, inhibition and direct reaction rate constants of NOM, respectively.

The pseudo-first order rate constant of ozone decomposition (k_{obs}) and the R_{ct} value for each addition of *tert*-butanol are measured. The values of k_i and k_s can be determined from the slope and intercept of the plot of $1/R_{ct}$ vs. $k_{SS}[S]$, respectively (Figure 1(a)) and those of k_p and k_D can be determined from the slope and intercept of the plot of k_{obs} vs. R_{ct} , respectively (Figure 1(b)). This method has been validated with model compounds and the rate constants of three NOM isolates were determined^{20, 21}.

^a Centre for Environmental Sustainability and Water Security, Faculty of Civil Engineering, Universiti Teknologi Malaysia, 81310 Skudai, Johor, Malaysia. Email: eeling@utm.my

^b Graduate Institute of Environmental Engineering, National Taiwan University, No. 1, Sec. 4, Roosevelt Road, Taipei 10617, Taiwan. Email: yipinlin@ntu.edu.tw*

* Electronic Supplementary Information (ESI) available: Effects of pH Value and Temperature on the Initiation, Promotion, Inhibition and Direct Reaction Rate Constants of Natural Organic Matter in Ozonation. See DOI: 10.1039/x0xx00000x

Nonetheless, the current development still lacks the fundamental understanding of the behavior of NOM at different pH and temperature. Although these two parameters have been extensively studied in the ozonation process, the information on their effects in the presence of NOM especially on the degradation of organic contaminants are generally limited and qualitative in nature. For instance, it was only known that the removal of organic contaminants in the ozonation process depended strongly on the presence of NOM^{23, 24}. While some contaminants showed effective degradation, those that are more ·OH-reactive were inhibited^{21, 25-29}. In addition, a change in pH and temperature can greatly influence the specific roles of NOM that affect the removal of organic contaminants but such effects have not been quantitatively reported. A detailed evaluation of the roles of NOM at different pH and temperature, therefore, is important to elucidate the effects of NOM on the degradation of organic contaminants in water ozonation under different environmentally-relevant circumstances.

The objective of this study was to apply the new method to investigate the influences of pH value and temperature on these rate constants of NOM in the ozonation process. The information can improve basic understandings of how NOM responds in terms of these reaction modes to the change of pH value and temperature that can affect the ozone exposure, ·OH exposure and contaminant removal. The rate constants determined at different temperatures allowed us to calculate the activation energy associated with each reaction mode to explore the thermodynamic characteristics of these NOM reactions. Suwannee River fulvic acid (SRFA), a well-characterized NOM isolate, was used as the model NOM.

2. Materials and Methods

2.1 Chemicals

All chemicals used in this study were of 98% purity or greater except for phosphoric acid which was 85% pure, and were used as received. Potassium indigo trisulfonate, *para*-chlorobenzoic acid (pCBA), sodium thiosulfate and *tert*-butanol were purchased from Sigma-Aldrich (USA). Hydrochloric acid (HCl), methanol, phosphoric acid, sodium hydroxide (NaOH), sodium hydrogen phosphate and sodium dihydrogen phosphate were supplied by Merck (Germany). All stock and experimental solutions were prepared using ultrapure water produced by Milli-Q Direct 8 Ultrapure Water Systems (Millipore, USA) with a resistivity of 18.2 mΩ cm. Ozone gas generated from pure oxygen by the Anseros ozone generator (Model COM-AD-02, Germany) was continuously sparged through a gas-washing bottle containing ultrapure water chilled in an ice bath to acquire fresh aqueous ozone stock solution³⁰. This generally yielded a concentration of approximately 60 mg/L of ozone. Suwannee River fulvic acid (SRFA, 2S101F) purchased from the International Humic Substances Society (IHSS) was dissolved in ultrapure water without pH adjustment and the solution was filtered with a 0.45µm pore size Whatman (UK) membrane filter before use. The measured carbon content and specific UV absorbance at 254 nm (SUVA₂₅₄) were 0.47 mg C per mg of SRFA and 5.5 L(mg C)⁻¹m⁻¹, respectively.

2.2 Experimental Methods

Prior to each experiment, the ultrapure water was pre-ozonated to minimize its ozone demand¹⁵. The pre-ozonated water was acidified with 1.0 M HCl to achieve a pH value of 3.5. The background dissolved inorganic carbon (bicarbonate/carbonate) which could react as an inhibitor was removed by purging the acidified water

with nitrogen gas²². A 1 L screw-top glass bottle equipped with a 10 mL bottle-top dispenser was utilized as the reaction vessel³¹.

Ozonation of NOM was initiated by adding ozone stock solution into experimental solutions containing phosphate buffer (1.0 mM), *tert*-butanol (0.03 to 0.3 mM), SRFA (2.0 mg/L), and the ·OH probe compound pCBA (0.5 µM) at various pH values (pH 6.5-8.0) and temperatures (12°C-50.5°C). Because of the low pCBA concentration employed in the experiments, its ·OH scavenging capacity was negligible²². The solution pH was adjusted to the desired pH value using 1.0 M NaOH and HCl under a gentle stream of nitrogen gas. The solution temperature was controlled by immersing the reaction vessel in a water bath connected to a water circulator (Polyscience 9100 series, USA). Samples were taken periodically from the reactor and quenched with indigo solution for ozone and sodium thiosulfate solution for pCBA measurements. The variations of pH value during the experimental period were within ±0.15 unit.

2.3 Analytical Methods

Ozone concentration in the stock solution was measured spectrophotometrically at 258 nm ($\epsilon = 3100 \text{ M}^{-1} \text{ cm}^{-1}$) and that in the experimental solution was determined using the Indigo method at 600 nm ($\epsilon = 20,000 \text{ M}^{-1} \text{ cm}^{-1}$)^{30, 32}. Both measurements were performed using a Shimadzu UV-1800 (Japan) spectrophotometer. Agilent 1200 series (USA) high performance liquid chromatography system consisting of a variable wavelength detector and Zorbax SB-C18 column (150 × 2.1 mm) was employed to determine the concentration of pCBA. pCBA was eluted using an isocratic mobile phase consisting of methanol (55%) and 10 mM phosphoric acid buffer (45%) at a flow rate of 0.2 mL/min and detected at 234 nm at 25°C²². The minimum detection limit of pCBA obtained from eight replicates was 0.004 µM. The pH value was measured using a Horiba pH meter (Japan) equipped with an Ag/AgCl pH electrode (Accumet, Cole-Palmer, USA) calibrated with pH 4.0, 7.0 and 10.0 standard buffers (Fisher Scientific, USA). Dissolved organic carbon (DOC) was quantified using the Shimadzu TOC-VCSH analyzer (Japan).

3. Results and Discussions

3.1 Effects of pH values

NOM is a heterogeneous macromolecule consisting of a variety of functional groups³³⁻³⁶. The change of pH value can result in the protonation/deprotonation of certain acidic functional groups and potentially affect the values of k_D , k_I , k_P , and k_S of NOM. Ozonation of NOM-containing water typically can be characterized as the initial rapid ozone decomposition and high R_{ct} stage (~20 s) followed by a relatively slow ozone decomposition and low R_{ct} stage^{20, 22, 37-39}. The two-stage ozone decomposition kinetics was also observed in our experiments (Fig S1[†]). Due to the limitation of the experimental setup in collecting data for the initial stage, the discussion in this paper was focused on the second stage.

Fig. 2 shows the plots of $1/R_{ct}$ vs. $k_{SS}[S]$ and k_{obs} vs. R_{ct} for pH 6.5 to 8.0 at 21±1 °C with the addition of 0.03-0.3mM of *tert*-butanol as the external inhibitor. Linear correlations were found for all pH conditions in both plots, corresponding well to the theoretical correlations shown in Fig 1. The values of k_I , k_S , k_P and k_D calculated from the slope and intercept for each pH value are summarized in Table 1. The value of k_I used in the calculation was $160 \text{ M}^{-1} \text{ s}^{-1}$ ^{20, 21}.

The value of k_I increased 5 times as pH value increased from 6.5 to 7.5 followed by a slight decline from pH 7.5 to 8.0, although the decrease was not statistically significant. Ozone selectively attacks electron-rich functional groups of a compound, such as olefins,

amines, and activated aromatic rings¹² which are ubiquitous moieties in the NOM macromolecule^{36, 40}. Free amines, deprotonated phenols as well as electron-rich aromatic components have been suggested to be the key moieties in NOM that react as initiators and contribute to the formation of $\cdot\text{OH}$ in ozonation^{9, 41}. In addition to $\cdot\text{OH}$ formation via electron transfer, the attack of ozone at the electron-rich aromatic components in NOM may also produce new phenols via the hydroxylation pathway, which has been suggested to be responsible for the continuing $\cdot\text{OH}$ production after the original reactive sites are consumed⁹. The pK_a values for simple phenols are typically greater than pH 9.5 except those with halogen and nitro substitutions. The pK_a values for protonated amines vary over a wider pH range¹². The complexity of NOM molecule could affect the pK_a values of the phenolic and amine groups in its structure. The deprotonated form of the acidic groups and the free amines possessed much greater rate constants with O_3 than their protonated counterparts, resulting in the so called "reactivity pK" phenomenon, i.e., a significant variation of rate constant can be observed even at the pH range much less than the pK_a values¹². The variation of k_i over the pH range investigated in this study, therefore, should be a collective result of the corresponding abundance of free amine and deprotonated phenolic groups and the "reactivity pK" phenomenon. It should be noted that some of these functional groups involving in the initiation reaction might be very reactive and consumed in the fast reaction stage (< 20 s)^{42, 43}, which could not be captured by the batch experimental procedures employed in this study.

The variation of k_p was not significant over the investigated pH range. It has been shown that compounds comprising aliphatic hydroxyl (including polyalcohols and sugars), carboxyl as well as aryl groups could react as promoters¹³, suggesting that these functional groups could be important moieties contributing to the promotion characteristics of NOM. The relative constant k_p determined at pH 6.5-8.0 should be a result of the similar reactivity of these functional groups toward $\cdot\text{OH}$ to form superoxide radical and ultimately another $\cdot\text{OH}$ at this pH range. It has been reported that aliphatic hydroxyacids such as hydroxymalonic acid reacts with $\cdot\text{OH}$ primarily via the abstraction of the carbon bound H atom to form $\cdot\text{OOC-C}(\text{OH})\text{-COO}\cdot$ radical and the rate is nearly constant at pH 6-10⁴⁴. In the presence of oxygen, $\cdot\text{OOC-C}(\text{OH})\text{-COO}\cdot$ radical can transform to hydroxyperoxyl radical ($\cdot\text{OOC-COO}(\text{OH})\text{-COO}\cdot$) and then release a superoxide radical⁴⁴. Similar reaction schematic may exist for tartaric acid⁴⁵. It should be pointed out that carboxylic group can also contribute to the inhibition reaction. Leitner and Dore (1996)⁴⁵ reported that $\cdot\text{OH}$ attacks unsubstituted carboxylic acids, such as malonic acid and succinic acid, primarily at the C-C bond and causes its cleavage without forming peroxy radicals, suggesting that the hydroxy substitution could be a crucial factor to make a carboxylic acid or similar moiety in the NOM molecule a potential promoter.

In general, the k_s value increased with the increasing pH value although the increment from pH 6.5 to 7.5 was not statistically significant. It is well established that simple molecules such as *tert*-butanol and acetate act as effective inhibitors, although under high concentrations they may partially contribute to the promotion reactions due to bimolecular decay of their peroxy radical formed from the reactions with $\cdot\text{OH}$ ^{44, 46}. Carboxylic, aliphatic hydroxyl and aryl groups could be important moieties responsible for the inhibition properties of NOM¹³. It is known that the rate constant of an acid with $\cdot\text{OH}$ generally is higher when the acid is deprotonated. For example, the rate constant of bicarbonate with $\cdot\text{OH}$ ($8.5 \times 10^6 \text{ M}^{-1} \text{ s}^{-1}$) is higher than that of carbonate ($4 \times 10^8 \text{ M}^{-1} \text{ s}^{-1}$)¹². The observed

increase of k_s as a function of increasing pH could be attributed to the deprotonation of the responsible acidic moieties in NOM.

The value of k_D was found to increase with the increasing pH value. It is known that olefins can react directly with ozone without $\cdot\text{OH}$ formation according to the Criegee mechanism¹². Aromatic compounds may also react directly with ozone contributing to the direct reaction pathway although it may be accompanied by a small yield of $\cdot\text{OH}$ ¹². These functional groups can contribute significantly to the direct reaction of NOM with ozone. When an acidic group is present, the deprotonated anion can supply additional electron density to C-C double bond and increase the rate of direct reaction due to the electrophilicity of ozone. The trend of a higher k_D at a higher pH should result from the deprotonation of acidic functional groups and the "reactivity pK" phenomenon described earlier.

It is interesting to compare k_i versus k_D , both resulting from the reactions of NOM with ozone and k_s versus k_p , both resulting from the reactions of NOM with $\cdot\text{OH}$. As shown in Table 1, k_D is 2.7-5.8 times higher than k_i , indicating that 73-85% of the reaction between SRFA and ozone proceeded via the direct reaction pathway, most likely for the cleavage of C-C double bond. k_p is 14-31 times higher than k_s , indicating that 93-97% of the reaction between SRFA and $\cdot\text{OH}$ proceeded via the promotion reaction pathway to form secondary organic radicals, in which superoxide radical can be formed in the presence of oxygen and reacts with additional ozone to ultimately generate another $\cdot\text{OH}$. The importance of promotion characteristics of NOM in accelerating ozone decomposition has been highlighted in ozonation of surface water³⁸ but its contribution has never been quantified. Using the described approach, the relative contribution of initiation and direct reaction of NOM toward ozone decay and that of promotion and inhibition toward $\cdot\text{OH}$ reaction can be quantitatively described.

The rate constant of the reaction between SRFA and $\cdot\text{OH}$ has been determined using electron pulse radiolysis to be $1.60\text{-}2.06 \times 10^8 \text{ L}(\text{mol C})^{-1}\text{s}^{-1}$ (or $1.33\text{-}1.72 \times 10^4 \text{ L}(\text{mg C})^{-1}\text{s}^{-1}$)^{47, 48}, which are between the inhibition and promotion rate constants obtained in this study. These rate constant are usually referred as the $\cdot\text{OH}$ "scavenging" rate constant and are useful in characterizing non-ozone based advanced oxidation processes. In ozonation, however, the "scavenging" reaction comprises both promotion and inhibition reactions, which must be distinguished to fully characterize the influences of NOM on the ozone decomposition and $\cdot\text{OH}$ formation that are important for quantifying the degradation of organic contaminants in water treatment. The rate constants determined in this study could fulfill these demands.

3.2 Effects of temperature

Fig. 3 shows the plots of $1/R_{ct}$ vs. $k_{SS}[S]$ and k_{obs} vs R_{ct} for temperature ranging from 12.0 to 50.5 °C with the addition of 0.03-0.3 mM of *tert*-butanol at pH 7.0. The ozone decomposition and R_{ct} plot are shown in Fig. S2†. The values of k_i , k_s , k_p and k_D of SRFA calculated from the slopes and intercepts of the two plots are summarized in Table 2. All rate constants of different reaction modes of SRFA increased with the increasing temperature. k_i exhibited the highest increment of 20-fold as the temperature increased from 12 °C to 50.5 °C, followed by k_D , k_s and k_p which increased by 13-, 9- and 4-fold, respectively.

The activation energy for each of the reaction modes can be determined from the Arrhenius equation as shown in Equation (3).

$$\ln(k) = -\frac{E_a}{R} \frac{1}{T} + \ln A \quad (3)$$

where E_a represents the activation energy, R represents the universal gas constant ($8.314 \text{ J mol}^{-1} \text{ K}^{-1}$), T represents the temperature in Kelvin and A is the pre-exponential factor.

According to the activated complex theory or transition-state theory, following relationships apply⁴⁹:

$$A = \frac{k_B T}{h} \times e^{\Delta S^\ddagger/R} \quad (4)$$

$$E_a = \Delta H^\ddagger + RT \quad (5)$$

$$\Delta G^\ddagger = \Delta H^\ddagger - T\Delta S^\ddagger = -RT \ln K^\ddagger \quad (6)$$

where k_B is the Boltzmann's constant ($1.38 \times 10^{-23} \text{ J K}^{-1}$), h is Planck's constant ($6.626 \times 10^{-34} \text{ J s}$), ΔS^\ddagger and ΔH^\ddagger are the change of entropy and enthalpy between the reactants and the activated complex, respectively, ΔG^\ddagger is the Gibbs free energy of activation, and K^\ddagger is the equilibrium constant of the activation.

It should be noted that the value of k_1 used in the calculation also depends on the temperature, which can be determined via the integrated form of Arrhenius equation as shown in Equation (7) if the activation energy for the reaction between ozone and $\cdot\text{OH}^\ddagger$ is known.

$$\ln\left(\frac{k_{1T_a}}{k_{1T_b}}\right) = \frac{E_a}{R} \left(\frac{1}{T_b} - \frac{1}{T_a}\right) \quad (7)$$

where a and b represent two different temperatures.

Based on the kinetics of ozone decomposition in pure water¹³, k_{obs} is directly proportional to k_1 value (Equation (8)).

$$k_{\text{obs}} = 3k_1[\text{OH}^\ddagger] \quad (8)$$

Therefore, the activation energy associated with k_1 should be equal to that associated with k_{obs} determined in pure water. Three activation energies determined in pure water were found in the literature: 76 ± 8.3 , 79.5 ± 8.0 and $82.5 \pm 8.0 \text{ kJ mol}^{-1}$ ^{50, 51}. The values of k_1 at different temperatures were computed using the average of the three activation energies, i.e. 79.3 kJ mol^{-1} . Our previous studies have found that k_1 was $160 \text{ M}^{-1} \text{ s}^{-1}$ at $21 \pm 1^\circ\text{C}$ ^{20, 21}. Employing this k_1 value and the average activation energy, k_1 values were calculated to be 57 , 490 , 1326 and $3083 \text{ M}^{-1} \text{ s}^{-1}$ for temperature at 12.0 , 31.5 , 41.5 and 50.5°C , respectively.

The Arrhenius plots for k_i , k_s , k_p and k_D are shown in Fig.4. Good linear correlations were found indicating that no significant configurational changes of SRFA structure over the temperature range studied⁴⁸. The determined E_a , $\ln A$, ΔS^\ddagger , ΔH^\ddagger , ΔG^\ddagger and K^\ddagger based on Equations (3)-(6) are summarized in Table 3. In general, we found distinct differences in ΔS^\ddagger , ΔG^\ddagger and K^\ddagger between the reactions involving ozone (direct reaction k_D and initiation reaction k_i) and those involving $\cdot\text{OH}$ (promotion reaction k_p and inhibition reaction k_s), indicating that different mechanisms and thermodynamic properties are involved in these two groups of reactions (i.e., the Criegee mechanism and ozone electron transfer vs. H-abstraction and $\cdot\text{OH}$ radical addition). The E_a for direct reaction and initiation reaction are 49.1 and 55.3 kJ/mol , respectively. These values are

comparable with those determined for simple organic compounds reacting with ozone^{12, 52-54}. The E_a for promotion and inhibition reactions are 25.6 and 50.1 kJ/mol . The difference could result from the different electron densities caused by the hydroxy substitution in the attacked carbon center that differentiates these two types of reaction modes. As discussed above, promotion reaction predominates inhibition reaction, which should reflect in the overall reaction between $\cdot\text{OH}$ and NOM. McKay et al. (2011)⁴⁸ reported that E_a for reaction of $\cdot\text{OH}$ with different NOM samples including SRFA ranges from 14.4 - 29.9 kJ/mol based on rate constants obtained using electron pulse radiolysis (E_a for SRFA = 14.4 kJ/mol). Although the promotion E_a for SRFA determined in this study is higher than the reported value, it falls in the range determined for NOM collected from different sources, signifying the important role of NOM as a promoter rather than an inhibitor in water ozonation.

3.3 Predicting the Degradation of Micropollutants in the Presence of NOM

Removal of micropollutants by ozonation can be affected by NOM, pH and temperature. The removal can be modeled using Equation (9) and (10) where the theoretical R_{ct} and k_{obs} can be obtained from Equation (1) and (2), respectively.

$$\left(\frac{[P]_t}{[P]_0}\right) = \exp(-(k_{\text{OH}/P}R_{\text{ct}} + k_{\text{O}_3/P})\int[\text{O}_3]dt) \quad (9)$$

$$\int[\text{O}_3]dt = \frac{[\text{O}_3]_0}{k_{\text{obs}}} (1 - e^{-k_{\text{obs}}t}) \quad (10)$$

where P denotes micropollutant, $k_{\text{OH}/P}$ and $k_{\text{O}_3/P}$ represent the second-order rate constant of $\cdot\text{OH}$ and O_3 with micropollutant, respectively, and $\int[\text{O}_3]dt$ is the ozone exposure.

Typically, $k_{\text{OH}/P}$ is in the order of $10^9 \text{ M}^{-1} \text{ s}^{-1}$ and $k_{\text{O}_3/P}$ can vary over several orders of magnitude. Owing to the limited rate constants of micropollutants at different temperatures, the simulation of their removal was only considered at different pH values. The effects of temperature, however, can be evaluated in the same fashion discussed below if required rate constants are available.

Six micropollutants including five pharmaceutical compounds (diazepam, N(4)-acetyl-sulfamethoxazole, bezafibrate, metoprolol and penicillin G) and a pulp bleach (zinc diethylenediaminetetraacetate), which have all been detected in surface waters were studied⁵⁵⁻⁶⁰. They were selected because of their $k_{\text{O}_3/P}$ were significantly different, varying over three orders of magnitude. Their pK_a and second-order rate constants with O_3 and $\cdot\text{OH}$ are shown in Table 4. 2 mg/L SRFA and 2 mM carbonate alkalinity were considered to mimic the real water condition. The modeling results are shown in Fig. 5 and the impacts of pH on their removal are summarized in Table 4. It should be noted again that these results represent the removal in the second R_{ct} stage.

The simulation indicated that the removal of diazepam was enhanced by the increasing pH value (Fig. 5 (a)). The small rate constant of ozone with diazepam ($k_{\text{O}_3/P} = 0.8 \pm 0.2 \text{ M}^{-1} \text{ s}^{-1}$) suggests that $\cdot\text{OH}$ is the main contributor to its removal. In fact, comparing its degradation due to $\cdot\text{OH}$ oxidation capacity ($k_{\text{OH}/P}R_{\text{ct}}\int[\text{O}_3]dt$)

and ozone oxidation capacity ($k_{O_3/p} \int [O_3] dt$), the latter can be neglected. According to Equation (1), the total initiation capacity ($2k_1[OH] + k_2[DOC]$) increased approximately 8-fold when pH increased from 6.5 to 8.0, in which at $< \text{pH } 7.0$ the contribution of OH^- to the total initiation capacity was less than 30%, i.e., more than 70% of the $\cdot OH$ was contributed by the initiation reaction of SRFA. As pH increased to 7.5 and 8.0, OH^- contributed 43% and 63% to the total initiation capacity. For zinc diethylenediaminetetraacetate, its removal was not affected by pH initially (< 400 s), thereafter, decreased with the increasing pH value. Although the $\cdot OH$ oxidation capacity increased 7 times as pH increased from 6.5 to 8.0, its contribution to the removal of zinc diethylenediaminetetraacetate at pH 8.0 was at most 39%, i.e., the removal due to ozone oxidation became significant due to the higher ozone rate constant ($k_{O_3/p} = 100 \text{ M}^{-1} \text{ s}^{-1}$). Similar trend was observed for N(4)-acetylsulfamethoxazole removal (Fig. 5(c)) but the differences among the four pH values became less significant because of its even higher rate constant with ozone ($k_{O_3/p} = 250 \text{ M}^{-1} \text{ s}^{-1}$). For bezafibrate (Fig. 5(d)), metoprolol (Fig. 5(e)) and penicillin G (Fig. 5(f)), increase in pH did not affect their removal as they can be predominantly removed by ozone ($k_{O_3/p} > 500 \text{ M}^{-1} \text{ s}^{-1}$). Although the results presented here are based on model simulation, the importances of understanding the kinetic behaviors of organic matter and the contribution of ozone and $\cdot OH$ to contaminant degradation have been demonstrated in experimental works¹¹.

4. Conclusions

NOM has long been known to simultaneously react as the initiator, promoter, inhibitor and direct ozone consumer in the ozonation process. Although the R_{ct} concept provides an empirical approach to characterize ozone exposure and $\cdot OH$ exposure, the lack of NOM rate constants for these reactions is one of the major obstacles to fully understand how NOM affects micropollutant degradation when ozone is used. In this study, the rate constants of NOM in these reactions at various pH values and temperatures were determined and used to investigate the thermodynamic characteristics of these reactions and model the removal of micropollutants. Future study can be devoted to determine the rate constants of NOM collected from different water sources (surface water, groundwater or even wastewater effluent), as well as their values in the initial stage (< 20 s) to provide a more thorough understanding of the behaviors of NOM and its impact on contaminant removal in the ozonation process.

Acknowledgements

The authors would like to acknowledge funding from Ministry of Science and Technology, Taiwan (NSC 102-2221-E-002 -243 -MY3), Ministry of Education, Malaysia (FRGS/1/2014/STWN01/UTM/02/8) and Universiti Teknologi Malaysia (Q.J130000.2609.10J26).

References

- C. W. Labatiuk, M. Belosevic and G. R. Finch, *Water Res.*, 1992, **26**(6), 733-743.
- J.L. Rennecker, B.J. Marinas, J.H. Owens and E.W. Rice, *Water Res.*, 1999, **33**(11), 2481-2488.
- S.A. Tyrrell, S.R. Rippey and W.D. Watkins, *Water Res.*, 1995, **29**(11), 2483-2490.
- N.K. Hunt and B.J. Marinas, *Water Res.*, 1997, **31**(6), 1355-1362.
- A. Driedger, E. Staub, U. Pinkernell, B. Marinas, W. Koster and U. von Gunten, *Water Res.*, 2001, **35**(12), 2950-2960.
- R. G. Rice, L. J. Bollyky and W.J. Lacy, *Analytical Aspects of Ozone Treatment of Water and Wastewater*. Lewis Publishers: USA, 1986.
- W.H. Glaze, *Environ. Sci. Technol.* 1987, **21**(3), 224-230.
- J.L. Acero, K. Stemmler and U. von Gunten, *Environ. Sci. Technol.*, 2000, **34**(4), 591-597.
- T. Nothe, H. Fahlenkamp and C. von Sonntag, *Environ. Sci. Technol.*, 2009, **43**(15), 5990-5995.
- J. Pablo Pocostales, M.M. Sein, W. Knolle, C. von Sonntag and T.C. Schmidt, *Environ. Sci. Technol.*, 2010, **44**(21), 8248-8253.
- Y. Lee, D. Gerrity, M. Lee, A.E. Bogeat, E. Salhi, S. Gamage, R.A. Trenholm, E.C. Wert, S.A. Snyder and U. von Gunten, *Environ. Sci. Technol.*, 2013, **47**(11), 5872-5881.
- C. von Sonntag and U. von Gunten, *Chemistry of ozone in water and wastewater treatment: From basic principles to applications*. IWA Publishing, London, UK, 2012.
- J. Staehelin and J. Hoigne, *Environ. Sci. Technol.*, 1985, **19**(12), 1206-1213.
- J. Hoigne and H. Bader, *Water Res.*, 1976, **10**, 377-386.
- J. Staehelin and J. Hoigne, *Environ. Sci. Technol.*, 1982, **16**(10), 676-681.
- U. von Gunten, *Water Res.*, 2003, **37**(7), 1443-1467.
- F.J. Stevenson, *Humus Chemistry: Genesis, Composition, Reactions*. John Wiley & Sons, New York, 1994.
- P. Westerhoff, R. Song, G.L. Amy and R. Minear, *Ozone Sci. Eng.*, 1997, **19**(1), 55-73.
- B. Langlais, D. A. Reckhow, and D.R. Brink, *Ozone in Water Treatment: Application and Engineering*. Lewis Publishers, USA, 1991.
- E.L. Yong and Y.P. Lin, *Water Res.*, 2012, **46**, 1990-1998.
- E.L. Yong and Y.P. Lin, *Ozone Sci. Eng.*, 2013, **35**(6), 472-481.
- M. Elovitz and U. von Gunten, *Ozone Sci. Eng.*, 1999, **21**, 239-260.
- J. Nawrocki and B. Kasprzyk-Hordern, *Appl. Catal. B-Environ.*, 2010, **99** (1-2), 27-42.
- B. Kasprzyk-Hordern, M. Ziolek and J. Nawrocki, *Appl. Catal. B-Environ.*, 2003, **46** (4), 639-669.
- P. Westerhoff, Y. Yoon, S. A. Snyder and E. C. Wert, *Environ. Sci. Technol.*, 2005, **39** (17), 6649-6663.
- R. Rosal, A. Rodriguez, M. S. Gonzalo and E. Garcia-Calvo, *Appl. Catal. B-Environ.*, 2008, **84** (1-2), 48-57.
- R. Rosal, M. S. Gonzalo, A. Rodriguez, and E. Garcia-Calvo, *J. Hazard. Mater.*, 2009, **169** (1-3), 411-418.
- F. J. Beltran, J. P. Pocostales, P. M. Alvarez and J. Jaramillo, *J. Hazard. Mater.*, 2009, **169** (1-3), 532-538.
- S. A. Snyder, E. C. Wert, D. J. Rexing, R. E. Zegers and D. D. Drury, *Ozone Sci. Eng.*, 2006, **28** (6), 445-460.
- H. Bader and J. Hoigne, *Water Res.*, 1981, **15**, 449-456.
- J. Hoigne and H. Bader, *Ozone Sci. Eng.*, 1994, **16**, 121-134.
- APHA; WWA; WEF, *Standard Methods For The Examination of Water and Wastewater*, 21st Ed. APHA, Washington DC, 2005.
- J.A. Leenheer, R.L. Wershaw and M. M. Reddy, *Environ. Sci. Technol.*, 1995, **29**, 393-398.
- J.A. Leenheer, R.L. Wershaw and M. M. Reddy, *Environ. Sci. Technol.*, 1995, **29**, 399-405.
- E.M. Thurman, *Organic geochemistry of natural waters*. Martinus Nijhof/Dr W. Junk, Dordrecht, 1985.

36. P. Westerhoff, J. Debroux, G. Aiken and G. L. Amy, *Ozone Sci. Eng.*, 1999, **21**(6), 551-570.
37. M. Elovitz, U. von Gunten and H. P. Kaiser, *Ozone Sci. Eng.*, 2000, **22**, 123-150.
38. J.L. Acero and U. von Gunten, *J. Am. Water Works Ass.*, 2001, **93**(10), 90-100.
39. M. O. Buffle, J. Schumacher, E. Salhi, M. Jekel and U. von Gunten, *Water Res.*, 2006, **40**(9), 1884-1894.
40. P. Westerhoff, G. R. Aiken, G.L. Amy and J. Debroux, *Water Res.*, 1999, **33**(10), 2265-2276.
41. M.O. Buffle and U. von Gunten, *Environ. Sci. Technol.* 2006, **40**(9), 3057-3063.
42. J. Hoigne and H. Bader, *Water Res.*, 1983, **17**, 185-194.
43. F. Munoz, and C. von Sonntag, *J. Chem. Soc., Perkin Trans. 2*, 2000, (10), 2029-2033.
44. M.N. Schuchmann, H.P. Schuchmann and C. von Sonntag, *J. Phys. Chem.*, 1995, **99**(22), 9122-9129.
45. N. K. V. Leitner and M. Dore, *J. Photoch. Photobio. A*, 1996, **99**(2-3), 137-143.
46. M.N. Schuchmann and C. von Sonntag, *J. Phys. Chem.*, 1979, **83**(7), 780-784.
47. P. Westerhoff, S.P. Mezyk, W.J. Cooper and D. Minakata, *Environ. Sci. Technol.*, 2007, **41**(13), 4640-4646.
48. G. McKay, M. M. Dong, J.L. Kleinman, S. P. Mezyk and F. L. Rosario-Ortiz, *Environ. Sci. Technol.*, 2011, **45**(16), 6932-6937.
49. W. Stumm and J.J. Morgan, *Aquatic Chemistry: Chemical Equilibria and Rates in Natural Waters*. 3rd Ed., John Wiley & Sons, Inc., Canada, 1996.
50. B.G. Ershov and P.A. Morozov, *Russ. J. Phys. Chem. A*, 2009, **83**(8), 1295-1299.
51. K. Sehested, H. Corfitzen, J. Holcman and J. E. Hart, *J. Phys. Chem.*, 1992, **96**, 1005-1009.
52. Y. Qiu, C. H. Kuo and M. E. Zappi, *Ozone Sci. Eng.*, 2007, **24**(2), 123-131.
53. K. E. Leather, M. R. McGillen, M. Ghalaieny, D. E. Shallcross and C. J. Percival, *Int. J. Chem. Kinet.*, 2011, **43** (3), 120-129.
54. A. M. Kharbuli and R. H. D. Lyngdoh, *J. Mol. Struct.-Theochem*, 2008, **860** (1-3), 150-160.
55. T. A. Ternes, *Water Res.*, 1998, **32**(11), 3245-3260.
56. Y. Yoon, J. Ryu, B. G. Choi and S.A. Snyder, *Sci. Total Environ.*, 2010, **408**, 636-643.
57. A. Y. C. Lin, T. H. Yu and C. F. Lin, *Chemosphere*, 2008, **74**, 131-141.
58. S. Castiglioni, R. Bagnati, R. Fanelli, F. Pomati, D. Calamari and E. Zuccato, *Environ. Sci. Technol.*, 2006, **40**, 357-363.
59. K. Stemmler, G. Glod and U. von Gunten, *Water Res.* 2001, **35**(8), 1877-1886.
60. M.C. Dodd, M. O. Buffle and U. von Gunten, *Environ. Sci. Technol.*, 2006, **40**(6), 1969-1977.
61. D.T. Manalack, *Perspect. Med. Chem.*, 2007, **1**, 25-38.
62. M. M. Huber, S. Canonica, G.Y. Park and U. von Gunten, *Environ. Sci. Technol.*, 2003, **37**(5), 1016-1024.
63. A. E. Martell and R. M. Smith, *Critical Stability Constants: Amino Acids*. Plenum Press: New York, 1989, Vol. 1.
64. E. Lee, S. Lee, J. Park, Y. Kim and J. Cho, *Drink. Water Eng. Sci.*, 2013, **6**, 89-98.
65. K. Fent, A. A. Weston and D. Caminada, *Aquat. Toxicol.*, 2006, **76**(2), 122-159.
66. J. Benner, E. Salhi, T. A. Ternes and U. von Gunten, *Water Res.*, 2008, **42**(12), 3003-3012.
67. F. J. Benitez, J. L. Acero, F. J. Real and G. Roldan, *Chemosphere*, 2009, **77**(1), 53-59.
68. W. Song, W. J. Cooper, S. P. Mezyk, J. Greaves, B. M. Peake, *Environ. Sci. Technol.*, 2008, **42**(4), 1256-1261.

Table 1 The second-order rate constants of initiation (k_i), inhibition (k_s), promotion (k_p) and direct ozone reaction (k_D) of SRFA at different reaction pH values. Values in the parenthesis indicate the standard deviation calculated from triplicate experiments. Experimental conditions: pH 6.5-8.0, initial ozone concentration = 0.1 mM, *tert*-butanol = 0.03 to 0.3 mM, pCBA = 0.5 μ M, phosphate buffer = 1.0 mM, and temperature = $21 \pm 1^\circ\text{C}$.

pH	k_i ($\text{L}(\text{mol C})^{-1}\text{s}^{-1}$)	k_s ($\text{L}(\text{mol C})^{-1}\text{s}^{-1}$)	k_p ($\text{L}(\text{mol C})^{-1}\text{s}^{-1}$)	k_D ($\text{L}(\text{mol C})^{-1}\text{s}^{-1}$)
6.5	0.64(± 0.03)	2.41(± 0.21) $\times 10^7$	7.54(± 0.66) $\times 10^8$	3.77(± 0.27)
7.0	1.53(± 0.29)	3.50(± 0.85) $\times 10^7$	8.32(± 0.92) $\times 10^8$	4.96(± 0.78)
7.5	3.01(± 0.09)	3.56(± 0.39) $\times 10^7$	8.37(± 0.82) $\times 10^8$	8.01(± 0.88)
8.0	2.37(± 0.68)	6.01(± 0.21) $\times 10^7$	8.44(± 0.90) $\times 10^8$	9.28(± 0.40)

Table 2 The second-order rate constants of initiation (k_i), inhibition (k_s), promotion (k_p) and direct ozone reaction (k_D) for 2.0 mg/L of SRFA at different temperature ranging from 12.0°C to 50.5°C. Experimental conditions: pH 7.0, initial ozone concentration = 0.1 mM, *tert*-butanol = 0.03 to 0.3 mM, pCBA = 0.5 μ M and phosphate buffer = 1.0 mM.

Temp (°C)	k_i (L(mol C) ⁻¹ s ⁻¹)	k_s (L(mol C) ⁻¹ s ⁻¹)	k_p (L(mol C) ⁻¹ s ⁻¹)	k_D (L(mol C) ⁻¹ s ⁻¹)
12.0	0.47(±0.03)	2.70(±1.30)×10 ⁷	7.24(±1.06)×10 ⁸	2.42(±0.06)
21.0	1.53(±0.29)	3.50(±0.85)×10 ⁷	8.32(±0.92)×10 ⁸	4.96(±0.78)
31.5	1.87(±0.31)	12.89(±5.22)×10 ⁷	12.42(±1.32)×10 ⁸	6.83(±0.64)
41.5	4.51(±0.84)	19.40(±2.54)×10 ⁷	13.42(±1.09)×10 ⁸	16.75(±2.31)
50.5	9.38(±1.50)	25.12(±4.73)×10 ⁷	29.66(±4.80)×10 ⁸	30.95(±9.21)

Table 3 Activation energy (E_a), pre-exponential factor ($\ln A$), entropy of activation (ΔS^\ddagger), enthalpy of activation (ΔH^\ddagger), Gibbs free energy of activation (ΔG^\ddagger) and equilibrium constant of the activation (K^\ddagger) of initiation (k_i), inhibition (k_s), promotion (k_p) and direct ozone reaction (k_D) rate constants for SRFA. Experimental conditions: pH 7.0, initial ozone concentration = 0.1 mM, *tert*-butanol = 0.03 to 0.3 mM, pCBA = 0.5 μ M and phosphate buffer = 1.0 mM, temperature = 12.0 to 50.5°C.

	E_a (kJ/mol)	$\ln(A)$	ΔS^\ddagger (J/K/mol)	ΔH^\ddagger (kJ/mol)	ΔG^\ddagger (kJ/mol)	K^\ddagger (M ⁻¹)
Direct reaction (k_D)	49.1±7.1	21.6±2.9	-73.9±21.4	46.6±7.0	68.8±13.4	(1.05±0.19)×10 ⁻¹²
Initiation (k_i)	55.3±4.8	22.7±2.0	-64.6±16.3	52.8±4.8	72.2±9.7	(2.71±0.32)×10 ⁻¹³
Promotion (k_p)	25.6±6.9	31.1±2.8	5.1±0.1	23.1±0.2	21.6±0.1	(1.74±0.88)×10 ⁻⁴
Inhibition (k_s)	50.1±2.6	38.1±0.8	63.5±6.6	47.6±2.9	28.5±0.9	(1.08±0.31)×10 ⁻⁵

Table 4 Influences of pH on the removal of selected pharmaceutical and organic compounds.

Compound	pK _a	k _{O₃/P} (M ⁻¹ s ⁻¹)	k _{OH/P} (M ⁻¹ s ⁻¹)	Impact of pH
Diazepam ^{61, 62}	3.4	(0.8±0.2)	(7.2±1.0)×10 ⁹	+
Zinc diethylenediaminetetraacetate ^{59, 63}	5.6, 6.1	100	(2.4±0.4)×10 ⁹	–
N(4)-acetylsulfamethoxazole ^{60, 64}	5.9	250	(6.8±0.1)×10 ⁹	+ (< 400 s); – (> 400 s)
Bezafibrate ^{62, 65}	3.6	(590 ±50)	(7.4±1.2)×10 ⁹	×
Metoprolol ⁶⁶⁻⁶⁸	9.7	1.4×10 ³	(8.4±0.1)×10 ⁹	×
Penicillin G ^{60, 61}	2.8	4.8×10 ³	(7.3±0.3)×10 ⁹	×

Note: +: enhance removal efficiency; – : inhibit removal efficiency; ×: no effect in removal efficiency

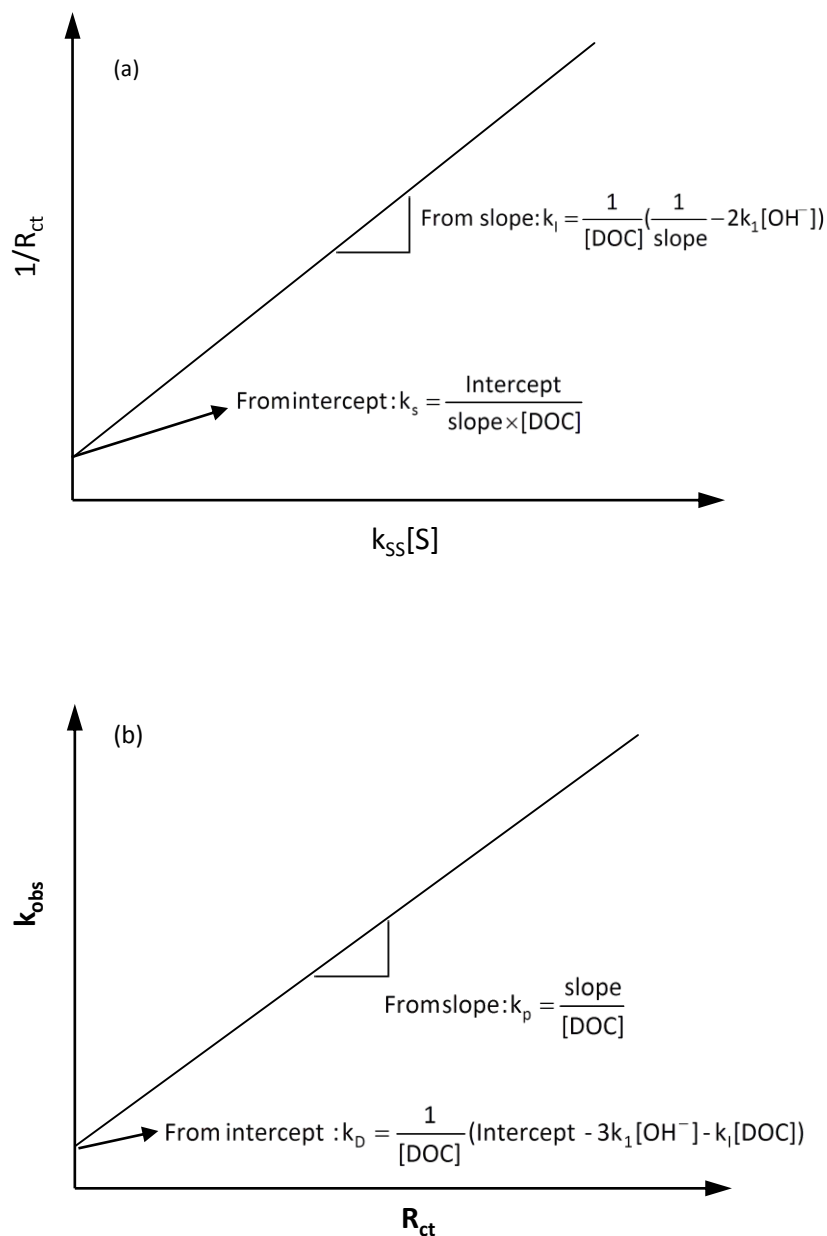


Fig. 1 Theoretical relationships of (a) $1/R_{\text{ct}}$ vs. $k_{\text{SS}}[\text{S}]$ and (b) k_{obs} vs. R_{ct} .^{20, 21}

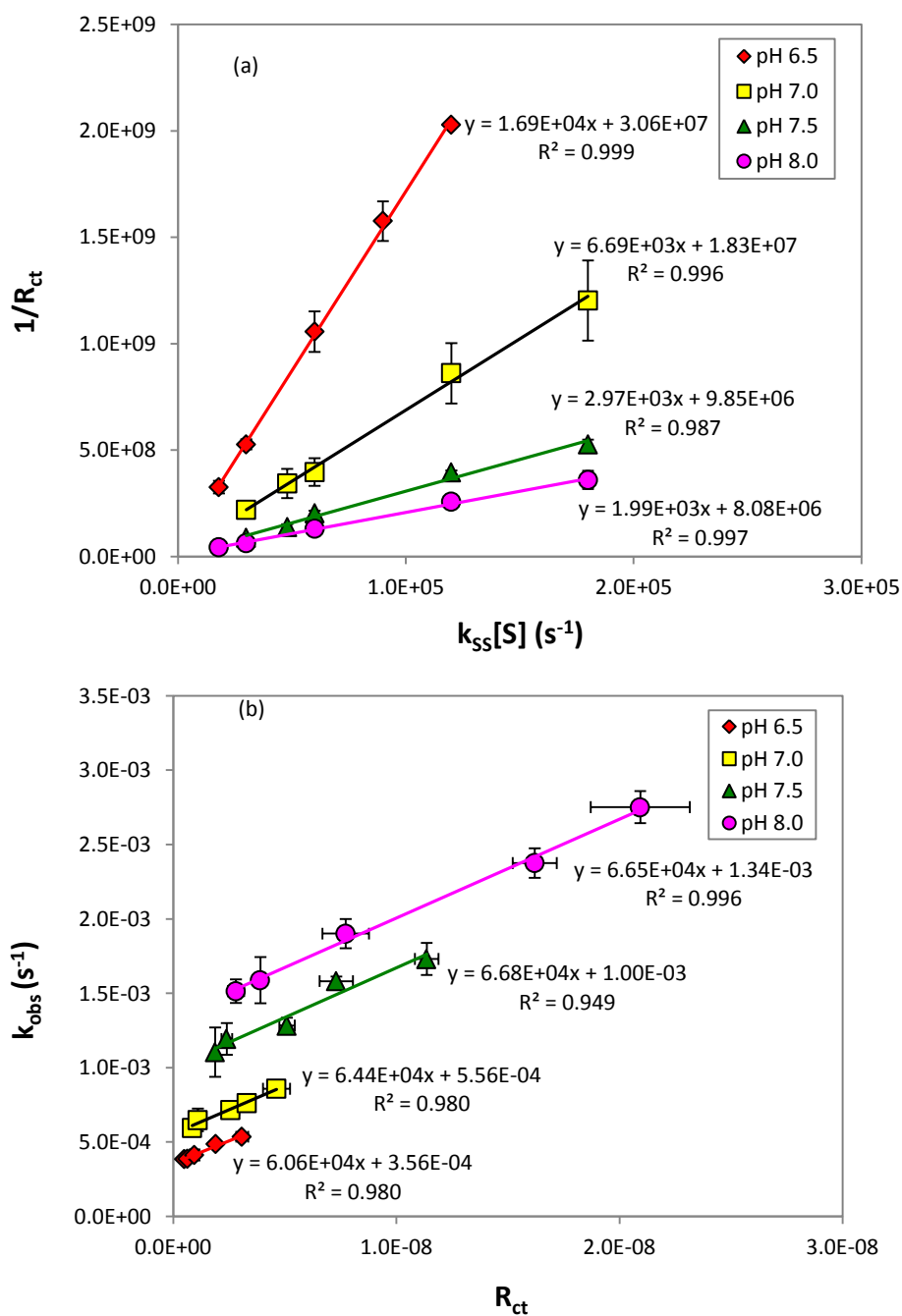


Fig. 2 (a) $1/R_{ct}$ vs $(k_{ss}[S])$ and (b) k_{obs} vs R_{ct} plots at various pH value (6.5-8.0). Experimental conditions: SRFA = 2.0 mg/L, temperature = $21 \pm 1^\circ\text{C}$, initial ozone concentration = 0.1 mM, *tert*-butanol = 0.03 to 0.3 mM, pCBA = 0.5 μM and phosphate buffer = 1.0 mM. The error bar represents the standard deviation obtained from triplicate.

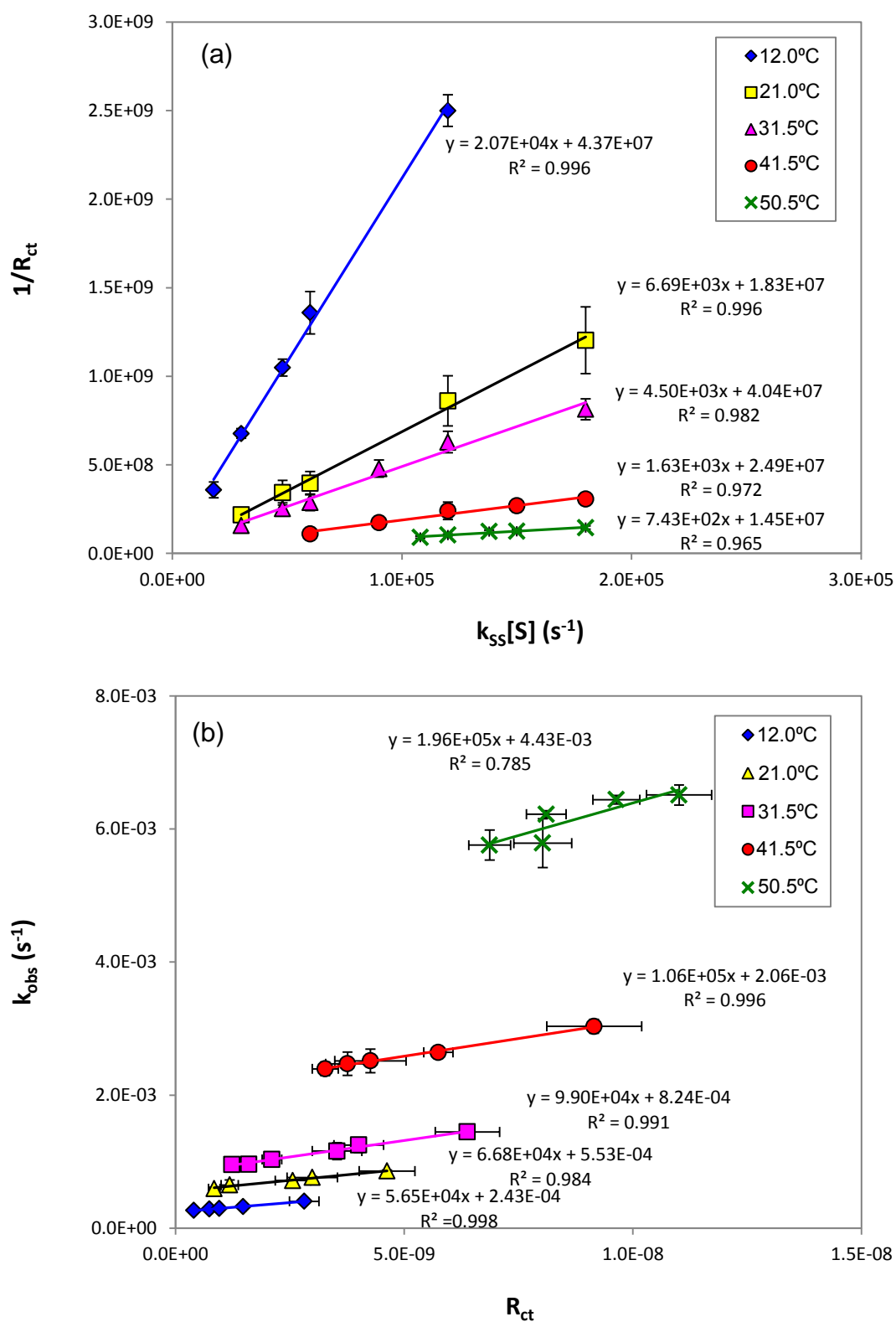


Fig. 3 The plots of (a) $1/R_{ct}$ vs $(k_{ss}[S])$ and (b) k_{obs} vs R_{ct} for 2.0 mg/L SRFA at temperature ranging from $12.0^{\circ}C$ to $50.5^{\circ}C$. Experimental conditions: pH 7.0, initial ozone concentration = 0.1 mM, *tert*-butanol = 0.03 to 0.3 mM, pCBA = 0.5 μ M and phosphate buffer = 1.0 mM. The error bar shows that the experiments were conducted in triplicate.

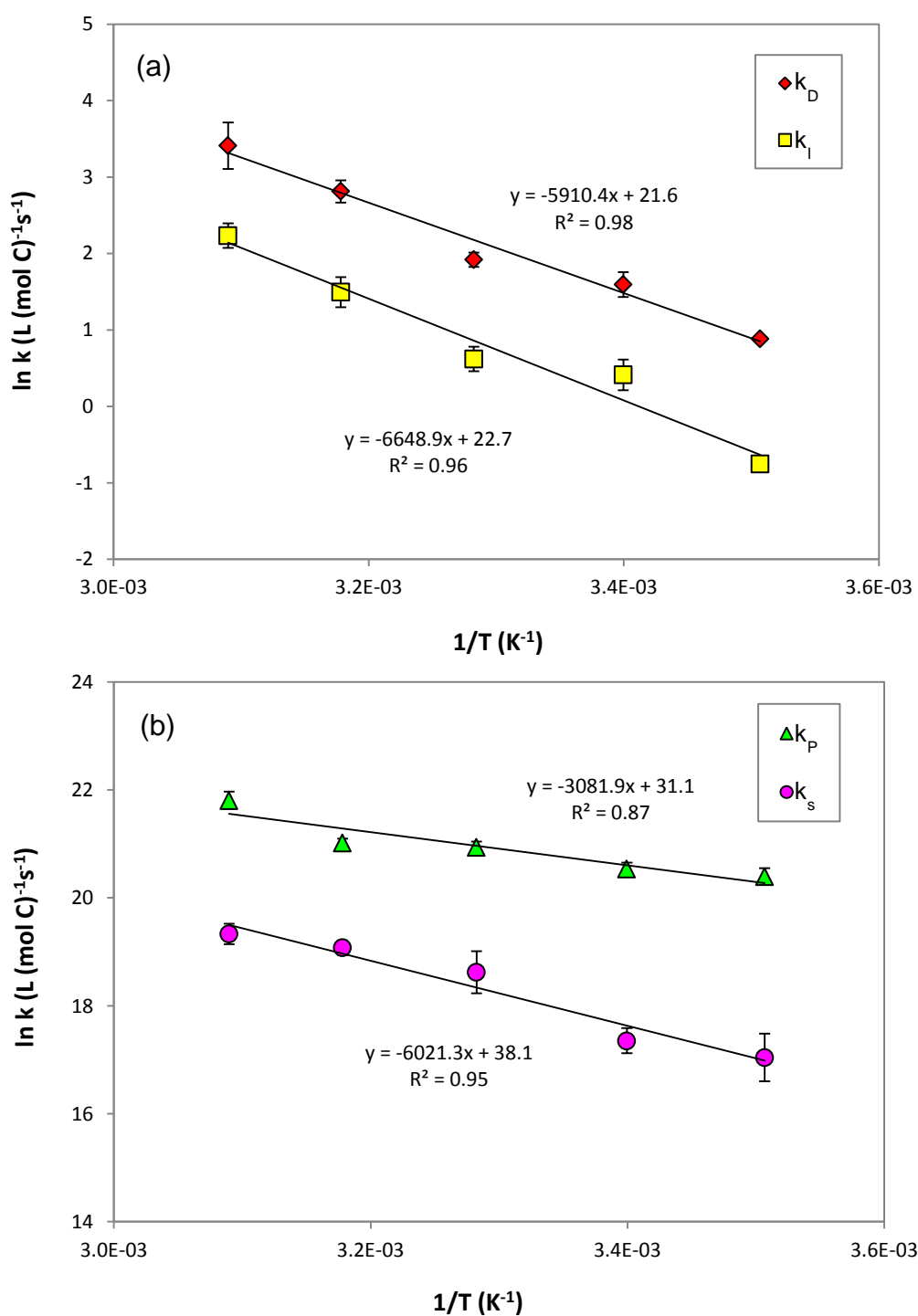


Fig. 4 Arrhenius plots for (a) direct reaction (k_D) and initiation (k_I) rate constants and (b) promotion (k_P) and inhibition (k_S) rate constants of 2.0 mg/L of SRFA at pH 7.0. Error bar represents the standard deviation obtained from triplicate experiments.

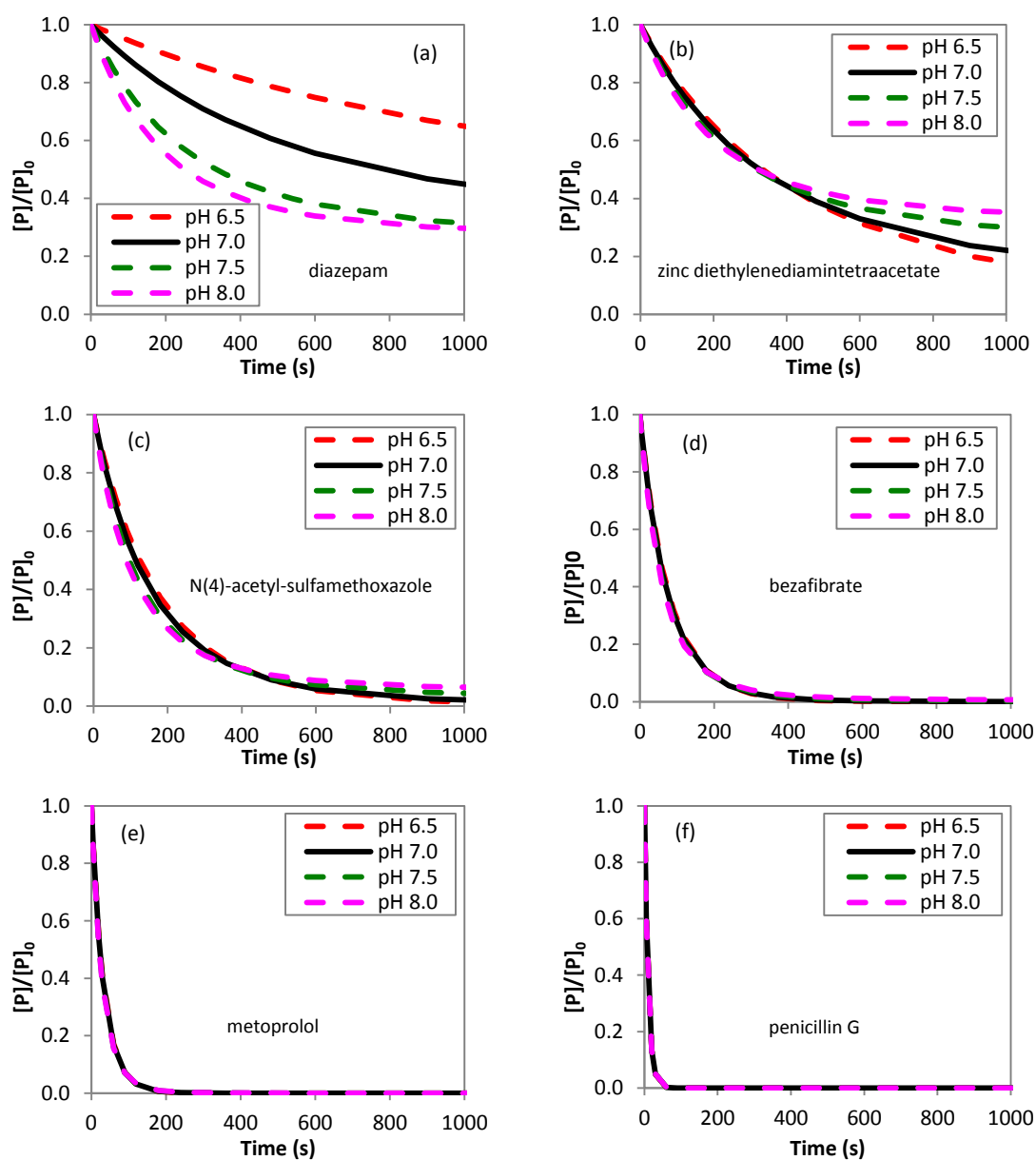
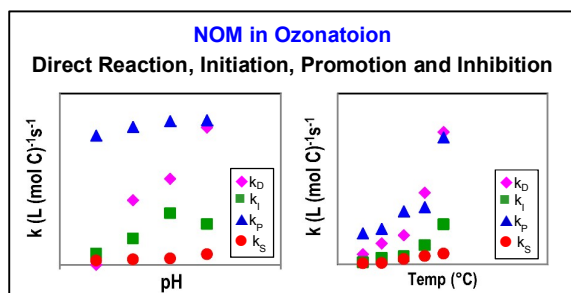


Fig. 5 Simulation of the removal of selected micropollutants, (a) diazepam, (b) zinc diethylenediaminetetraacetate, (c) N(4)-acetyl-sulfamethoxazole, (d) bezafibrate, (e) metoprolol and (f) penicillin G, in the presence of 2.0 mg/L SRFA. Ozonation conditions: pH 6.5-8.0, initial ozone concentration = 0.021 mM, carbonate alkalinity = 2 mM, $[P] = 0.5 \mu\text{M}$.

Graphical Abstract



pH and temperature affect the kinetics of specific reactions of NOM and influence organic contaminants removal in the ozonation process.